

*Ligand binding and unfolding of tryptophan synthase revealed by ion mobility-tandem mass spectrometry employing collision and surface induced dissociation*

**Royston S. Quintyn, Mowei Zhou, Shai Dagan, John Finke & Vicki H. Wysocki**

**International Journal for Ion Mobility Spectrometry**

ISSN 1435-6163  
Volume 16  
Number 2

Int. J. Ion Mobil. Spec. (2013) 16:133-143  
DOI 10.1007/s12127-013-0126-4



**Your article is protected by copyright and all rights are held exclusively by Springer-Verlag Berlin Heidelberg. This e-offprint is for personal use only and shall not be self-archived in electronic repositories. If you wish to self-archive your article, please use the accepted manuscript version for posting on your own website. You may further deposit the accepted manuscript version in any repository, provided it is only made publicly available 12 months after official publication or later and provided acknowledgement is given to the original source of publication and a link is inserted to the published article on Springer's website. The link must be accompanied by the following text: "The final publication is available at [link.springer.com](http://link.springer.com)".**

# Ligand binding and unfolding of tryptophan synthase revealed by ion mobility-tandem mass spectrometry employing collision and surface induced dissociation

Royston S. Quintyn · Mowei Zhou · Shai Dagan ·  
John Finke · Vicki H. Wysocki

Received: 19 November 2012 / Revised: 5 February 2013 / Accepted: 13 February 2013 / Published online: 23 March 2013  
© Springer-Verlag Berlin Heidelberg 2013

**Abstract** Understanding protein tertiary and quaternary structures is crucial to a better understanding of their biological functions. Here we illustrate for tryptophan synthase that tandem mass spectrometry (MS/MS) reveals not only protein subunit architectures, but also protein unfolding behavior when coupled with ion mobility (IM). In the present study, we verified the subunit arrangement with surface

induced dissociation (SID). We are able to correlate experimental results by IM with those obtained in unfolding simulations for the hetero-tetramer Tryptophan Synthase (TS) protein complex by identifying the presence of at least three stable intermediates ( $I_1$ ,  $I_2$ , and  $I_3$ ) during the unfolding process in collision induced dissociation (CID). We illustrate that the unfolding of the TS complex is likely due to the initial unfolding of an  $\alpha$ -monomer subunit, followed by the unfolding of the second  $\alpha$ -monomers. We also illustrate the ability of this combination of techniques to not only identify conformational changes of TS upon addition of D,L- $\alpha$ -glycerol phosphate (GP), but also to determine the location of the ligand, which is buried within the  $\alpha$ -monomer of the TS.

**Electronic supplementary material** The online version of this article (doi:10.1007/s12127-013-0126-4) contains supplementary material, which is available to authorized users.

R. S. Quintyn · M. Zhou · S. Dagan · V. H. Wysocki  
Department of Chemistry and Biochemistry,  
University of Arizona, 1306 E. University Blvd., PO Box 210041,  
Tucson, AZ, USA

J. Finke  
Department of Chemistry, Oakland University,  
260 Science and Engineering Building,  
Rochester, MI, USA  
e-mail: jfinke@uw.edu

*Present Address:*

R. S. Quintyn · M. Zhou · V. H. Wysocki (✉)  
Department of Chemistry and Biochemistry, Ohio State University,  
484 W. 12th Ave.,  
Columbus, OH, USA  
e-mail: wysocki.11@chemistry.ohio-state.edu

*Present Address:*

S. Dagan  
Israel Institute for Biological Research (IIBR), POB 19,  
Ness Ziona 74100, Israel

*Present Address:*

J. Finke  
Interdisciplinary Arts and Sciences, University of Washington  
Tacoma, UW Tacoma Campus Box 358400,  
1900 Commerce Street,  
Tacoma, WA 98402-3100, USA

**Keywords** Tryptophan synthase · Ligand binding · Protein unfolding · Conformational change · Surface induced dissociation · Ion mobility

## Introduction

Tryptophan Synthase (TS) is a hetero-tetrameric bienzyme complex ( $\alpha_2\beta_2$ ), comprised of two  $\alpha$  and two  $\beta$  subunits that catalyzes the final two steps in the biosynthesis of L-tryptophan [44,51]. The two  $\beta$  subunits (molecular weight=43 kDa each) exist as a dimer, with the two  $\alpha$  subunits (molecular weight=29 kDa each) flanking the  $\beta_2$  dimer. Hence, the quaternary structure of TS has an extended, nearly linear  $\alpha\beta\beta\alpha$  subunit arrangement [30]. In the first step of the biosynthesis of L-tryptophan, indole-3-glycerol phosphate (IGP) is cleaved to produce glyceraldehyde 3-phosphate (G3P) and indole at the active site of the  $\alpha$  subunit [53]. Indole is then transferred to the  $\beta$  active site via a 25 Å channel located along the inside of  $\beta$  subunit [43,51,59], where it reacts with L-serine in a pyridoxal

5'-phosphate (PLP)-dependent reaction to produce L-tryptophan [53]. Fluorescence, X-ray crystallography and enzyme-linked immunosorbent assay (ELISA) studies have shown that the presence of these ligands result in conformational changes of TS [13,15,44].

TS belongs to a ubiquitous class of proteins known as the Triosephosphate Isomerase (TIM) enzymes [54]. Generally, proteins must adopt a specific folded three-dimensional structure in order to be biologically active [12] and all proteins belonging to the TIM class show no exception to this rule. TIM enzymes all have a TIM barrel fold, which is comprised of eight repeating folds with each consisting of one  $\alpha$ -helix and one  $\beta$ -strand, such that eight parallel  $\beta$ -strands on the inside are covered by eight  $\alpha$ -helices on the outside [65]. A search of the Protein Data Bank indicates that the TIM barrel fold is the most common scaffold [65] and understanding this fold has been the topic of extensive research [8,17,18,65]. It should also be noted that extensive research has not been limited to the TIM barrel protein fold, but protein folding in general [12,24,26,42,46,62]. The kinetic process of a protein folding into its native state is not random [37]; it is believed that protein folding occurs from the fully unfolded state to the native state via a number of kinetic intermediates [34]. The formation of one or several highly populated stable unfolded intermediates is characteristic of the TIM class of proteins [54]. This stability is due to the fact that segments of the  $(\alpha/\beta)_8$  multi-domain can unfold through a stepwise process [12], with certain domains unfolding individually [50], either independently or with varying degrees of interactions between them [9,25]. An evaluation of protein folding studies has shown that these intermediates can be identified using two approaches [11]. The first involves monitoring the kinetic intermediates formed during both folding and unfolding, as the folding pathway is not necessarily the reverse of the unfolding pathway. The second involves characterizing the thermodynamically stable intermediates formed during unfolding initiated by employing denaturing conditions [11]. Many studies have employed both approaches to determine the intermediates present in TS. In one such study, refolding of the urea-denatured  $\alpha$ -subunit of TS ( $\alpha$ -TS) was monitored by pulse-quench hydrogen exchange mass spectrometry [67]. Not only did this study reveal the presence of multiple intermediates, but it also showed that the thermodynamic stability and kinetic accessibility of one of the intermediates favors a folding pathway in which the intermediate is an obligatory species in the folding of  $\alpha$ -TS [67].

The ability to study proteins in the gas-phase has been made possible by the development of electrospray ionization (ESI) [19], which allows for the charging of intact proteins, as they are transferred from solution-phase into the gas-phase [48]. With the advent of nanoelectrospray ionization (nano-ESI) [66], which generates smaller droplets, thereby resulting in less disruption to non-covalent interactions, mass spectrometry (MS) analysis has been extended to protein complexes

[27]. Within recent years native mass spectrometry has emerged as a vital tool in studying protein structural assemblies. Native mass spectrometry allows for the investigation of intact protein complexes with high sensitivity and a theoretically unrestricted mass range [27]. Although MS only provides low-resolution structural data such as oligomeric state, its major advantage over other tools such as nuclear magnetic resonance (NMR) and X-Ray crystallography is that MS is capable of interrogating samples at low concentrations and in mixtures in real time [12,29,61]. The reason MS is such a promising tool for the analysis of protein complexes is due to the ability to simultaneously detect multiple populations of protein assemblies [61]. A recent investigation illustrates this fact - the researchers employed nano-ESI MS, together with an automated mass spectrum analysis algorithm, to study the resulting architecture and interaction formed between small Heat Shock Proteins (sHSP) and their target proteins [63].

Despite the capabilities of MS in determining the stoichiometry of intact protein complexes [28], the determination of spatial relationships between constituent subunits in a protein complex is significantly more challenging [14]. One common approach to determining protein complex topology is the partial or complete dissociation of non-covalent complexes in solution, into their individual subunits via adjustment of pH or ionic strength [38]. Alternatively, the use of tandem-mass spectrometry (MS/MS) allows for dissociation of protein complexes in the gas-phase [14]. The most common activation method used in tandem MS is collision-induced dissociation (CID). In low-energy CID, the complex undergoes a multitude of collisions with neutral gas atoms or molecules, which typically results in restructuring of the complex, unfolding of a monomer and subsequent dissociation to give a highly charged monomer and its complementary low charge state (n-1)-mer product ion [4,5] - although a few exceptions have been reported [16,64]. As a result, CID often provides limited information regarding the subunit arrangement of protein complexes. An alternative activation method is surface-induced dissociation (SID), in which ions collide into a surface target often composed of a fluorinated alkanethiol self-assembled monolayer [32]. In SID, the product ions are characterized by a more charge-symmetric behavior, where charge is proportionally distributed among product ions based on their mass [3,32,68]. The lower-charged SID product ions are more compact than the highly charged CID product ions [69]. Consequently, SID offers a better means of identifying subunit arrangement in protein complexes. This has been shown in a previous study from our group on a heterohexameric complex, toyocamycin nitrile hydratase (TNH). In that study, it was illustrated that SID of TNH produces constituent  $\alpha\beta\gamma$  trimers, which are believed to arise due to the fact that SID is a high-energy, fast deposition process [6], allowing the structurally informative faster cleavage pathway to outcompete the slower monomer unfolding dissociation pathway.

While a lower charged product ion may be indicative of a subunit being more compact, the limitation of  $m/z$  information in isolation is that one can only speculate on conformation of the proteins based on charge state. A recent addition to native mass spectrometry is ion mobility (IM), which gives information about shape and conformation of protein complexes and addresses the limitation of isolated  $m/z$  information [39,55,56]. Native MS combined with IM not only allows for the determination of subunit composition and protein complex topology [55,56,58], but also can be used to study subunit unfolding in protein complexes [21,22,57]. Integrating experimentally measured collisional cross section (CCS) with CCSs calculated for structures proposed by molecular modeling also enhances the ability of native MS coupled with IM to determine the architecture of protein complexes [49].

Results reported in literature that were based on investigation of the  $\alpha$ -TS subunit with a variety of tools such as Hydrogen-Deuterium Exchange (HDX) MS [54], x-ray crystallography [53], equilibrium simulations [20], optical spectroscopy [44] and urea-gradient gel electrophoresis [40] provided useful context for this present work, which is a three-part IM-MS/MS investigation of the  $\alpha_2\beta_2$  tetrameric TS complex. In the first part of this present investigation, the topology of TS was investigated by selecting the tetrameric complex and subsequently activating it via SID. Secondly, CID activation was coupled to IM to monitor the CCS of the tetrameric complex to ascertain the number of intermediates present during the unfolding process. In the final part of this study, D,L- $\alpha$ -glycerol phosphate (GP) cofactor was added to the complex and a conformational change was determined by monitoring the CCS of the tetrameric complex. The complex, with ligand present, was then activated via CID and SID as a means of not only characterizing the  $\alpha$ -monomer ions produced by both methods, but also to determine whether GP was present in the active site of the  $\alpha$ -monomer.

## Experimental methods

Tryptophan Synthase was purchased from Sigma-Aldrich (St. Louis, MO, U.S.A.). To achieve native TS complexes, sample as purchased was diluted to a concentration of 100  $\mu\text{M}$  (because of the high  $K_d$  of TS), except when the spontaneous dissociation of tetrameric TS to produce “native-like” trimer was encouraged by diluting native TS to a concentration of 25  $\mu\text{M}$ . Subsequently, the protein samples were buffer exchanged into 100 mM ammonium acetate buffer (pH=7.8) with size exclusion chromatography spin columns (Bio-Rad, Hercules, CA, U.S.A.). In a few of the experiments, a solution of 100 mM triethylammonium acetate (TEAA) was added to native TS protein samples to

produce charge reduced TS. In the ligand-mediated conformational study, L-Serine was added to a 100  $\mu\text{M}$  TS sample (control) and L-Serine and D,L- $\alpha$ -glycerol phosphate (GP) were added to a 100  $\mu\text{M}$  TS sample (ligand-bound TS), followed by buffer exchange using the same conditions as mentioned before. The concentrations of L-Serine and GP used were 20 mM and 40 mM respectively, which were the limits before ion suppression occurred.

Mass spectrometry analysis was carried out utilizing a modified Quadrupole-Ion Mobility-Time of Flight (Q-IM-TOF) instrument (Synapt G2, Waters Corporation, Manchester, UK) with a customized SID device installed before the IM chamber [69]. Operation of the instrument in this set-up has been previously described [69]. In all experiments, a capillary voltage of 1.0–1.5 kV and a cone voltage of 50 V were employed in nanoelectrospray. No heating was applied to the cone. Procedures of nano-ESI glass capillary and surface preparation can be found elsewhere [23]. Instrumental conditions used were 5 mbar for the source/backing pressure, 2 mbar for nitrogen gas pressure in the IM cell, 120  $\text{mL min}^{-1}$  gas flow into the helium cell,  $\approx 6 \times 10^{-7}$  mbar in the TOF analyzer, and a wave velocity and height of 200  $\text{ms}^{-1}$  and 20 V respectively for IM. Travelling wave (T-wave) IM experiments reported in literature have illustrated that optimization of instrumental parameters and calibration standards are crucial for obtaining accurate T-wave CCS values [60]. In preparation of the calibration curve, T-Wave CCS values were determined at five combinations of T-wave velocities and wave heights (200  $\text{ms}^{-1}$  & 15 V, 200  $\text{ms}^{-1}$  & 18 V, 200  $\text{ms}^{-1}$  & 20 V, 300  $\text{ms}^{-1}$  & 20 V and 400  $\text{ms}^{-1}$  & 20 V) for all standards. The averaging of CCS values from measurements of native-like protein standards under several T-wave conditions with high  $R^2$  have been shown in the literature [60] to generate good CCS measurements that are comparable with drift tube measurements. Therefore, in the present work, CCS calibration curves were generated following a published protocol [10], using four protein complexes as standards with a mass range that bracketed the mass of the analyte- transthyretin tetramer, concanavalin A tetramer, serum amyloid P pentamer and glutamate dehydrogenase hexamer. A comparison of the CCS values obtained utilizing the five wave conditions (200  $\text{ms}^{-1}$  & 15 V, 200  $\text{ms}^{-1}$  & 18 V, 200  $\text{ms}^{-1}$  & 20 V, 300  $\text{ms}^{-1}$  & 20 V and 400  $\text{ms}^{-1}$  & 20 V) indicated that there was a standard deviation of <1 %. Hence, for the measurement of the difference in CCS with and without ligand, all five wave conditions were used. However, all other T-wave IM experiments were carried out utilizing a wave velocity of 200  $\text{ms}^{-1}$  and a wave height of 20 V because these conditions maximized the  $R^2$  of the calibration plot ( $R^2$  0.9991). Voltages in the instrument were tuned to ensure that extra activation was minimized without compromising the transmission of ions. Crystal structures of the  $\alpha$ -monomer

(1V7Y),  $\beta_2$ -dimer (1X1Q) and  $\alpha\beta$ -dimer with and without ligand (1BKS and 2RHG) were obtained from the Protein Data Bank. The two  $\alpha\beta$ -dimers were combined in PyMOL to produce the  $\alpha_2\beta_2$  tetramer. The same was done with the  $\alpha$ -monomer and  $\beta_2$ -dimer to form the  $\alpha\beta_2$ -trimer. Hydrogen atoms were then added to the crystal structures and the theoretical CCS values were calculated directly by using the open source software MOBCAL. The data produced by MOBCAL is based on three models, which calculate the theoretical CCS of a molecule using its three-dimensional coordination file [41]. In this research, the Exact Hard Spheres (EHS) model [41] was employed. It has been reported in literature that the Projection Approximation (PA) method does not address the effects of multiple collisions, and hence for ions of masses greater than 2 kDa, this method underestimates CCSs and is of limited value for larger bio-molecules [33]. The Trajectory Method (TM) is not optimized and was found to be computationally too challenging for the larger proteins and thus failed. The MOBCAL calculations were performed on the high performance computing servers at the University of Arizona.

## Results and discussion

### Topology of the tetrameric tryptophan synthase $\alpha_2\beta_2$ complex

The TS  $\alpha\beta\beta\alpha$  complex has two types of interfaces; the  $\alpha\beta$  interface and the  $\beta\beta$  interface. The  $\alpha\beta$  interface is hydrophobic in nature, with an area of approximately  $1,190 \text{ \AA}^2$  of the  $\alpha$  subunit interacting with an area of  $1,110 \text{ \AA}^2$  of the  $\beta$  subunit [30] and a dissociation constant ( $K_d$ ) of  $2.2 \times 10^{-5} \text{ M}$  [2]. The two  $\beta$  subunits interact over an area of  $1,440 \text{ \AA}^2$  via several forces, van der Waals hydrophobic, hydrogen bonding, and ion pair interactions, with a  $K_d$  as low as  $3.7 \times 10^{-10} \text{ M}$  [30]. Clearly, the  $\beta\beta$  interface is much more stable than the  $\alpha\beta$  interface. Figure 1 (a and b) shows representative CID and SID MS/MS spectra for the +27 tetrameric TS complex respectively. CID of the TS complex produces  $\alpha$ -monomers and their complementary  $\alpha\beta_2$ -trimers, whereas SID resulted in a different dissociation pattern. In addition to  $\alpha$ -monomers and  $\alpha\beta_2$ -trimers, SID also yielded  $\beta$ -monomers and  $\beta_2$ -dimers, which were not observed under CID. This is not surprising, given that SID is a fast process that deposits more energy in the TS complex than CID. CID is a multistep, slower process [3,32] so SID results in more product ions as there is sufficient energy available to access a variety of dissociation channels, including disrupting the stronger  $\beta\beta$  interface.

An examination of the  $\alpha$ -monomers produced by CID and SID reveals that CID  $\alpha$ -monomers show a broad range of charge states (+6 to +18) with gradually increasing CCS (Fig. 1c) which is characteristic of monomer unfolding. Conversely, SID produced  $\alpha$ -monomers that show a smaller

range of lower charge states (+5 to +11) that do not change in CCS in the lower charge states but increase at higher charge states, +8 and higher (Fig. 1d). Note that a given charge state is either compact or elongated regardless of activation method used. Further examination of Fig. 1c and d shows that while the higher proportion of CID  $\alpha$ -monomer product ions are unfolded, most of them remain compact in SID. These observations are in line with the investigation of CCS of the activated but undissociated tetramer with increasing acceleration voltage (Fig. 2a and b), where the extent of unfolding seen in SID is much less than in CID.

Prior studies have shown that charge-reduced protein assemblies retain compact conformations before activation [7]; [47]. Analyses were carried out on charge-reduced TS tetrameric complex to determine whether TS would produce “native-like” product ions as seen in SID for typical charging seen in ammonium acetate. The term “native” or “native-like” is used to describe a product ion that has a CCS value similar to that calculated for its corresponding crystal structure in MOBCAL. The extent of unfolding is indeed markedly reduced in both CID and SID of charge reduced precursors (Fig. 2c and d), although the same number of unfolding intermediates can still be distinguished in CID. In CID, the total change in CCS of the +19 tetramer is approximately  $2100 \text{ \AA}^2$ , which is much less than that seen for the +27 tetramer ( $\sim 3700 \text{ \AA}^2$ ), whereas in SID, the +19 tetramer remains intact before it dissociates. Consequently, the CID  $\alpha$ -monomer product ions obtained from the +19 tetramer are not as unfolded as those obtained from the +27 tetramer, whereas the SID  $\alpha$ -monomer product ions from the +19 tetramer remain mostly compact (see Figure S1a and S1b in the Supporting Information).

This behavior, where CID and SID produce predominantly unfolded and folded monomers respectively, is similar to results of a recent study by our group, which examined the CCS of the dominant CID and SID monomers produced from a number of protein complexes, namely C-Reactive Protein (CRP), Transthyretin (TTR) and Serum Amyloid P (SAP) [69]. It was found that the CCS values of SID monomers were similar to the values calculated for clipped “native” monomers. Conversely, a majority of CID monomers unfolded with increasing charge state, although some compact monomers were observed at low charge states. A comparison of “native” monomers produced in both activation methods, showed that “native” CID products existed in a lower abundance than seen in SID [69].

An investigation of the complementary  $\alpha\beta_2$ -trimers (Fig. 1e and f) reveals similar results. The CID  $\alpha\beta_2$ -trimer product ions show a broad range of charge states (+10 to +21), with increasing CCS as the charge state increases (Fig. 1e). Conversely, the SID  $\alpha\beta_2$ -trimer product ions show a narrower range of lower charge states (+9 to +13) which exist predominantly as compact structures (Fig. 1f). As was the case for the  $\alpha$ -monomer product ions, the higher

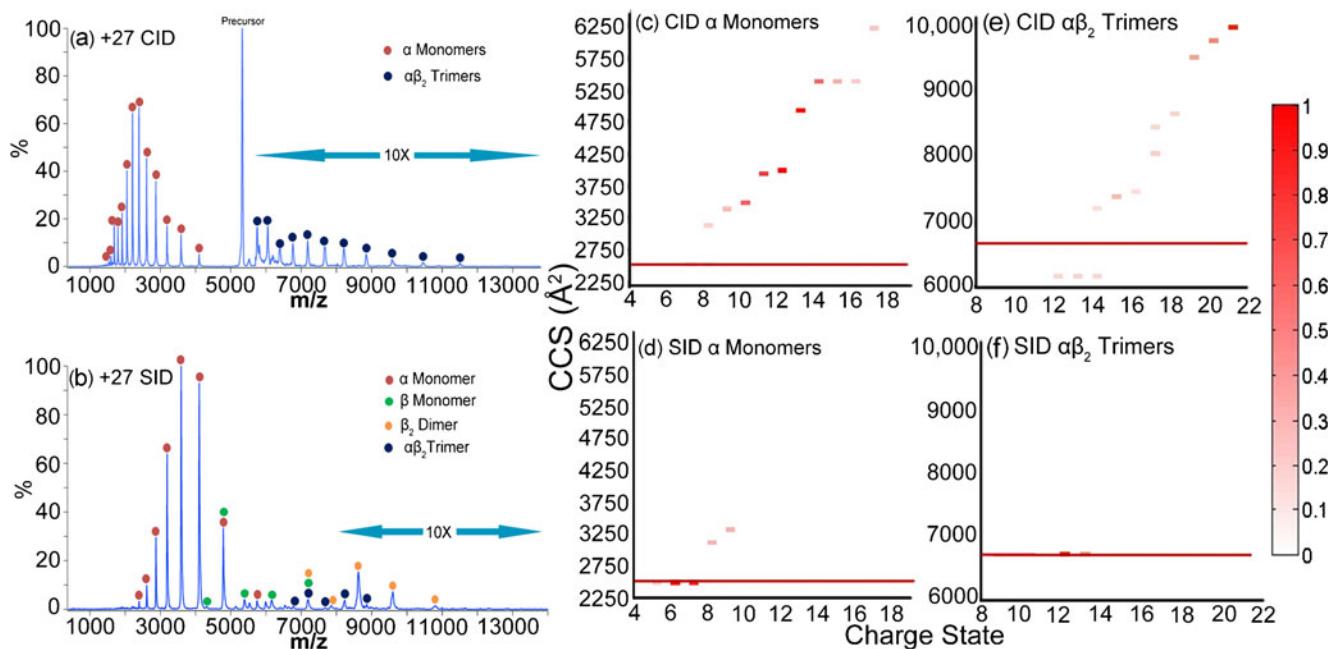


**Fig. 1** Dissociation products of the +27 TS heterotetramer complex precursor obtained from nano-ESI MS/MS at an acceleration voltage of 100 V. Representative (a) CID and (b) SID spectra are shown. CCS of monomer (c–d) and trimer (e–f) products are shown for both CID and SID. The red line indicates the CCS of the native products (native

trimers were clipped from TS tetramer) determined from Mobcal. As indicated on the color bar, *white* represents no product present, whereas the deepest *red* represents the highest abundance of product present. As shown, CID and SID products exist predominantly in the unfolded and folded states respectively

proportion of CID  $\alpha\beta_2$ -trimer product ions exists in unfolded states, while the SID  $\alpha\beta_2$ -trimer product ions remain folded. However, further examination of the CCS of various charge states of both the CID and SID  $\alpha\beta_2$ -trimers product ions reveals an interesting phenomenon, where it is

observed that the lower charge state  $\alpha\beta_2$ -trimer product ions show a CCS value lower than that calculated based on the crystal structure ( $\sim 500 \text{ \AA}^2$  smaller in both cases). A lower CCS value ( $\sim 200 \text{ \AA}^2$  smaller) than was expected based on the crystal structure was also seen in the  $\beta_2$ -dimer product

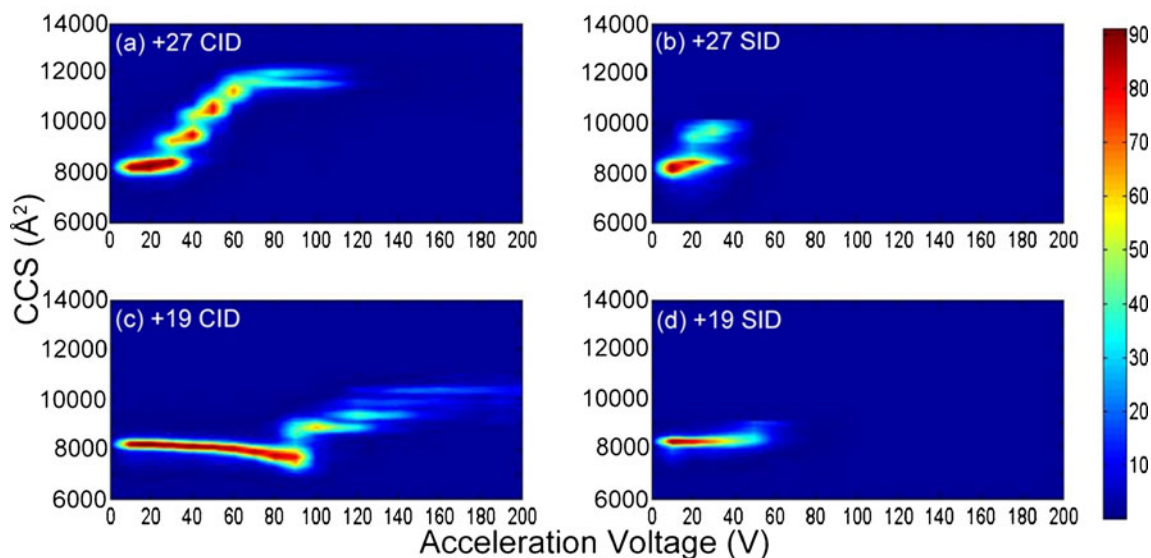


**Fig. 2** Dependence of CCS and survival of TS tetramer precursor on acceleration voltage. Experiments were performed by increasing the acceleration voltage and monitoring the changes in drift time (which were converted to CCS) of the fraction of precursor remaining, using

nano-ESI-MS/MS-IMS. As indicated by the color bar, *blue* represents a low abundance of precursor, while *red* represents a high abundance. In CID, remaining TS tetramer precursor unfolds; whereas in SID, the remaining precursor remains mostly folded as dissociation occurs

ions (see Figure S2b in the Supporting Information). No such change was seen for either the  $\alpha$ -monomer or the  $\beta$ -monomer product ions. Moreover, the CCS values observed for the  $\beta$ -monomers are similar to those calculated based on the crystal structure (see Figure S2a in the Supporting Information). This observation may have been realized as it has been reported that not only is the binding site for the coenzyme PLP buried within the interfaces between the  $\beta$ -structural domains, but also conformational changes involving substantial decrease in exposed hydrophobic surfaces are observed upon binding PLP or  $\alpha$ -chains [52]. Hence, we propose that the reason a CCS value lower than was expected was observed in both  $\beta_2$ -dimer and  $\alpha\beta_2$ -trimer product ions, may be due to a collapse of the “hydrophobic” active site in the  $\beta_2$ -dimer upon collisional activation due to the absence of the co-enzyme- PLP. This “collapse” was also seen in the +19 tetramer (Fig. 2c), where a decrease of  $\sim 550 \text{ \AA}^2$  was observed. However, such a change was not seen in the +27 tetramer (Fig. 2a). The fact that a collapse is not seen in the +27 tetrameric TS complex can be attributed to the charge repulsion effect caused by the additional eight charges, which may have made it difficult for a collapse to occur.

#### Multistate unfolding of the tetrameric TS $\alpha_2\beta_2$ complex

Figure 2a and c also reveal the presence of a number of intermediates during the unfolding process of the TS tetrameric complex. To investigate the multistate unfolding of TS, the +27 tetrameric precursor (two  $\alpha$ -subunits present) and a +22  $\alpha\beta_2$ -trimeric precursor (only one  $\alpha$ -subunit present) obtained from the solution distributions of the TS complex were selected and activated via CID while their CCS was monitored as a function of the collision voltage. Charge density affects the extent of unfolding as shown by the different unfolding profiles for the +19 and +27 tetramers. The charge densities of the +27 tetramer and +22 trimer are approximately  $+27/8200 \text{ \AA}^2$  and  $+22/6600 \text{ \AA}^2$  respectively. Hence, the +27 tetramer and +22 trimer were chosen because they have similar charge densities, thus allowing for a more accurate comparison. The results of this analysis are shown in Fig. 3. Figure 3a and b both show the presence of three intermediates ( $I_1$ ,  $I_2$  and  $I_3$ ) in the +27 tetrameric TS complex and the +22  $\alpha\beta_2$ -trimer respectively. In both the tetramer and trimer, the acceleration voltages at which the three intermediates occur were similar with  $I_1$ ,  $I_2$  and  $I_3$  appearing at 40 V, 50 V and 60 V, respectively. The unfolded state also appears at the same acceleration voltage (70 V) in both tetramer and trimer. Because both the +27  $\alpha_2\beta_2$ -tetramer and the +22  $\alpha\beta_2$ -trimer have similar charge densities, the fact that these voltages are similar for both allows us to propose that the same bonds are being broken in both the tetramer and trimer. One plausible explanation for this similar behavior is that the three intermediates formed

must have discrete structures in specific regions of both tetramer and trimer as they unfold. A comparison of the experimental CCS values obtained for the SID  $\alpha$ -monomer (See Fig. 1d) and  $\beta_2$ -dimer (See Figure S2b) product ions indicates that while a small amount of unfolding of the  $\alpha$ -monomer is observed, the  $\beta_2$ -dimer remains compact. From the fact that the  $\beta_2$ -dimer remains compact, it can be surmised that the tetrameric TS complex unfolds due to unfolding of the  $\alpha$ -monomer, supported by the different charge state distributions observed for the  $\alpha$ -monomer product ions obtained from the +27 tetrameric TS complex at 40 V, 50 V and 60 V (See Figure S3a in Supporting Information). These gas-phase findings are consistent with solution reports on the unfolding of the  $\alpha$ -subunit of TS ( $\alpha$ -TS), which have also shown the presence of a number of intermediates [20,54]. In one such study, urea-induced unfolding of the  $\alpha$ -subunit of TS, monitored using HDX-MS and circular dichroism determined that the  $\alpha$ -subunit unfolds via two stable equilibrium intermediates, of which the first retains a significant fraction of the native ellipticity [54]. In another study, temperature-induced unfolding simulations of the  $\alpha$ -subunit reveal the presence of two intermediate ensembles,  $I_1$  and  $I_2$ , during unfolding/refolding at the folding temperature,  $T_f=335 \text{ K}$ .  $I_1$  demonstrates discrete structure in regions  $\alpha_0$ - $\beta_6$  whereas  $I_2$  is a loose ensemble of states with an N-terminal structure varying from at least  $\beta_1 - \beta_3$  (denoted  $I_{2A}$ ) to  $\alpha_0 - \beta_4$  (denoted  $I_{2B}$ ) [20]. This present study illustrates that unfolding of the  $\alpha$ -subunit upon activation of the TS complex and the  $\alpha\beta_2$ -trimer behaves similarly to the  $\alpha$ -subunit when it exists as an independent entity in solution.

An examination of the changes in CCS of the tetramer and trimer relative to their initial states shows that while the CCS changes seen in  $I_1$  for both tetramer and trimer are practically the same, this is not the case for  $I_2$ ,  $I_3$  and the unfolded states (as indicated in the plot in Fig. 3c). In a previous study, the unfolding behavior of a heterodimer  $\alpha\beta$ -Spectrin bound laterally lengthwise- an architecture similar to the  $\alpha_2\beta_2$  TS complex- was monitored using Atomic Force Microscopy (AFM) [36]. Results from that study indicate that there was an equal probability of one monomer unfolding or both monomers unfolding simultaneously, based on where the AFM tip was placed. The  $\alpha_{20-21}/\beta_{1-2}$  lateral interaction was found to be much stronger than that of  $\alpha_{18-19}/\beta_{3-4}$ , thus forming a strong and weak affinity component within the dimer complex. Attachment of the tip to the weaker end resulted in the unfolding of single chains, whereas attaching it to the stronger end resulted in the simultaneous unfolding of both chains within the dimer [36]. In this present study, it is apparent that there is a comparatively larger CCS change observed for the tetrameric complex than that of the trimer, except in the case of the first intermediate when the change is similar. Consequently,

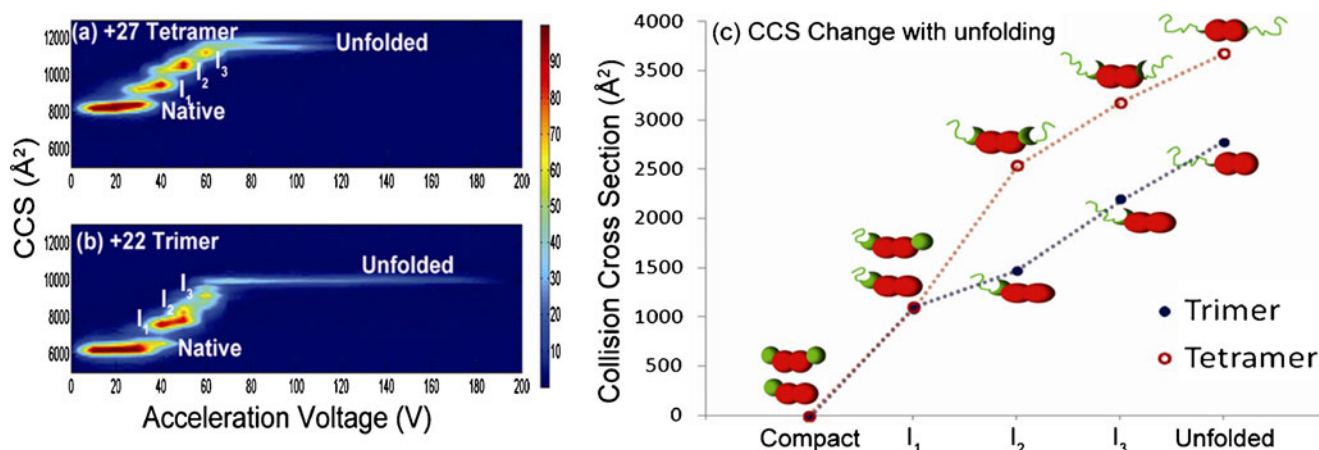


**Fig. 3** Unfolding of TS tetramer and trimer under CID. +27 TS tetramer was obtained by spraying 100  $\mu\text{M}$  TS in 100 mM  $\text{NH}_4\text{OAc}$ , whereas +22 TS trimer was obtained by spraying 25  $\mu\text{M}$  TS in 100 mM  $\text{NH}_4\text{OAc}$ . Both (a) tetramer and (b) trimer

we propose that initially at a lower collision voltage, one of the terminal exposed ends of the  $\alpha$ -monomer subunits unfold independently ( $I_1$ ). As the collision voltage is increased, both  $\alpha$ -monomer subunits unfold simultaneously, as the stronger end of the  $\alpha$ -monomer subunit, i.e. the segment at the  $\alpha\beta$  interface, unfolds ( $I_2$  and  $I_3$ ). The proposed unfolding pathway of both trimer and tetramer can be seen to the right of the plot in Fig. 3c.

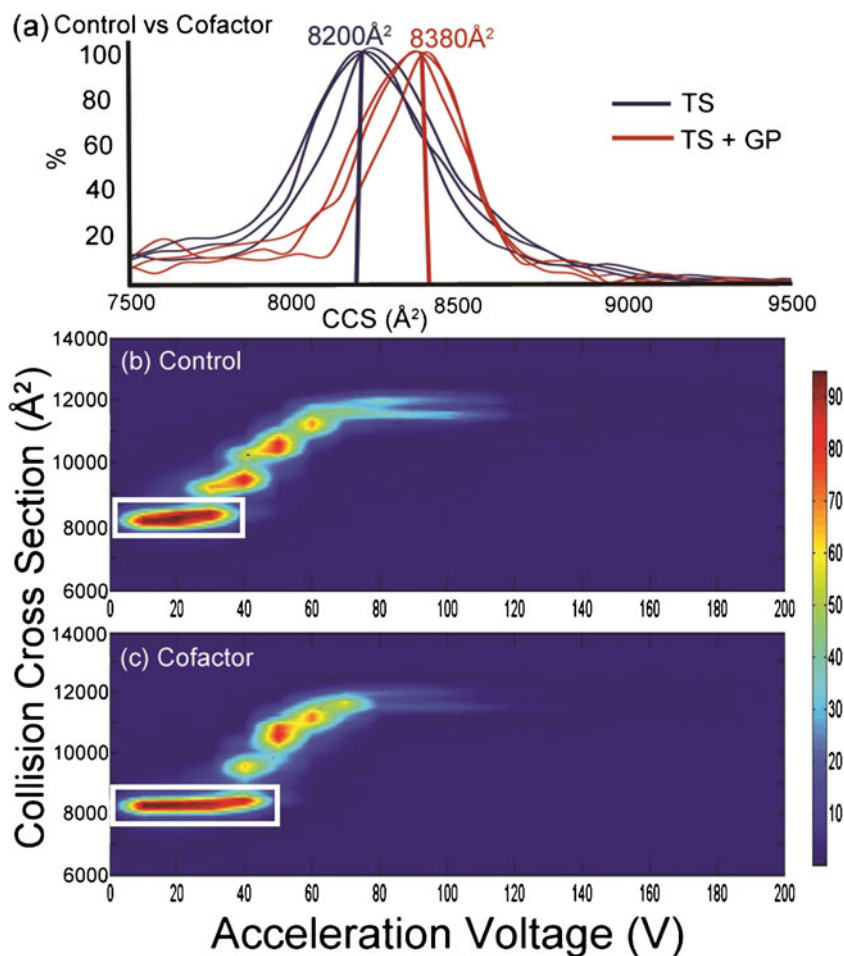
#### Ligand mediated conformational changes

As alluded to earlier, the  $\alpha$ -subunit catalyzes the reversible retro-aldol cleavage of indole-3-glycerol phosphate (IGP) to produce glyceraldehyde 3-phosphate (G3P) and indole [51]. X-ray crystallography has shown that upon addition of a ligand, the flexible loop located next to the active site moves from an “open” to “closed” conformation, effectively covering the active site. In the closed conformation, the hydroxyl group of  $\alpha\text{Thr183}$  in loop 6 is believed to interact with the  $\text{O}\delta$  of  $\alpha\text{Asp60}$  in loop2, thereby positioning the carboxylate of  $\alpha\text{Asp60}$  for hydrogen bond formation with the indole nitrogen of IGP [53]. It has also been shown that binding of the phosphate apparently induces large conformational and positional changes in nearby residues, especially in Gly234 and Ser235 [30]. Whereas the addition of IGP results in the  $\alpha$ -subunit attaining a “completely closed” conformation, the addition of G3P results in the  $\alpha$ -subunit having a “partially closed” conformation that mimics the transition-state for IGP cleavage. [15] Ngo et al. also revealed that the binding of ligands at the active site of the  $\alpha$ -subunit triggers a conformational change in the  $\beta$ -site to a state with an increased affinity for L-Ser. [45] Hence, in the present study, GP, a common non-reactive analogue of G3P was added to the tetrameric TS complex in the presence of

unfold via a three-intermediate pathway. Plot (c) shows the change in CCS of all forms of both tetramer and trimer, relative to their corresponding native state

excess L-Serine and the CCS of the complex was monitored to determine if there was a conformational change. L-Serine was also added to the TS complex in the absence of GP, so any change in CCS that is seen can be interpreted as due to binding of GP to the active site. Mobcal calculations indicated that the addition of GP resulted in a change in CCS of  $180 \text{ \AA}^2$ . A comparison of the CCS of the TS complex with and without ligand at a low acceleration voltage of 10 V CID (Fig. 4a) at various wave conditions shows that there is an average increase in CCS of approximately  $170 \text{ \AA}^2$ , which is near the known/applied bin size of  $180 \text{ \AA}^2$ , when GP is added. In a typical ion mobility measurement in the Synapt G2 instrument, ions are pulsed into the time of flight analyzer two hundred times (200 bins), which limits measurements of ions to discrete drift times, and thus the CCS of ions can only have discrete values. By varying the wave conditions, we were not only able to determine the optimum wave conditions for this experiment, but we were able to ascertain the reproducibility of the experimental CCS value. While the CCS/bin varied minimally with varying wave conditions ( $200 \text{ ms}^{-1}$  & 15 V,  $200 \text{ ms}^{-1}$  & 18 V,  $200 \text{ ms}^{-1}$  & 20 V,  $300 \text{ ms}^{-1}$  & 20 V and  $400 \text{ ms}^{-1}$  & 20 V), the average CCS obtained from these experiments for TS without ligand was  $8200 \text{ \AA}^2 \pm 0.24 \%$ , while in the presence of the ligand the average CCS was  $8380 \text{ \AA}^2 \pm 0.24 \%$ . Thus, the average change in CCS was  $180 \text{ \AA}^2 \pm 20 \text{ \AA}^2$ . Hence, the change in CCS upon addition of ligand was reproducible, when employing various wave conditions. Consequently, this present study confirms that there is a conformational change that accompanies the addition of GP to the TS complex. Figures 4b and c show the results of an IM-MS unfolding “fingerprint” experiment, where the population and CCS of the tetrameric TS complex is monitored as the acceleration voltage is increased. While the five states observed during the

**Fig. 4** Ligand induced conformational change. Experiments were performed by adding 20 mL-Serine (Control) and 20 mM L-Serine and 40 mM GP (Cofactor) to 100  $\mu$ M TS in 100 mM  $\text{NH}_4\text{OAc}$  and monitoring the changes in drift time (which was converted to CCS) as well as fraction of precursor remaining with increasing acceleration voltage using nano-ESI-MS/MS-IMS. (a) The CCS of tetramer with (red) and without GP (blue) at a CID acceleration voltage of 10 V at various wave conditions (wave velocity was held constant at  $200 \text{ ms}^{-1}$ , while wave height was changed as follows: 15 V, 18 V & 20 V). Change in CCS of tetramer b) without GP and c) with GP as acceleration voltage increases. When GP is added, not only is there a small shift in CCS of the native state, but it also persists over a greater range of acceleration voltages. These changes are highlighted by a white box



unfolding process of TS without GP are conserved upon addition of GP (See Figure S4 in Supporting Information), the “native-like” CCS of the tetrameric TS complex persists to higher acceleration voltages upon the addition of GP (See Fig. 4b and c). These results parallel previously reported transthyretin (TTR) results where IM-MS unfolding “fingerprint” studies reveal stability differences upon addition of thyroxine (its natural ligand) to the protein complex[31]. A review on computational methods to predict binding free energy in ligand-receptor complexes illustrated that conformational changes that accompany binding of a ligand to a protein complex involve the burial of hydrophobic surfaces so as to enhance binding [1]. The active site of the  $\alpha$ -subunit of TS is comprised of a number of hydrophobic amino acids, such as Phe22, Gly211, Gly213 and Gly234 and two polar residues-Tyr175 and Ser235 [30]. The burial of the hydrophobic amino acids may have caused these amino acids to be closer to each other resulting in the formation of new non-covalent interactions. This rearrangement may not only explain the conformational change, but also the enhanced stability of the “native-like” form of the TS complex observed.

An analysis of the CCS of the beta dimers produced (+9, +10 and +11) with GP and without GP illustrate no

change in CCS upon addition of the ligand. This indicates that there was no significant conformational change in the beta dimer upon addition of ligand, which was expected as GP does not bind to the active site of the beta dimer. Binding studies employing spectrophotometric titration and equilibrium dialysis reveal that there is only one binding site per equivalent of  $\alpha$ -subunit [35]. Figure 5 shows the  $\alpha$ -monomer region of representative MS/MS CID and SID spectra at 100 V with and without GP. An examination of the spectra illustrates that some peaks exist as doublets. From charge state deconvolution, it is apparent that these peak pairs represent the  $\alpha$ -monomer without GP and with one GP molecule present. Further examination also reveals that in both CID and SID, the CCS change between peak pairs, based on differences in drift time, is comparable with the change seen with ligand binding, and is only present in folded or partially-folded  $\alpha$ -monomers. Hence, we propose that in the unfolded  $\alpha$ -subunit, the residues present in the active site are no longer in close proximity and therefore GP can no longer bind to the  $\alpha$ -subunit. This experiment also shows that even as unfolding occurs, the  $\alpha$ -monomer products retain some amount of discrete structure. A comparison of the spectra obtained for CID and SID, when GP is

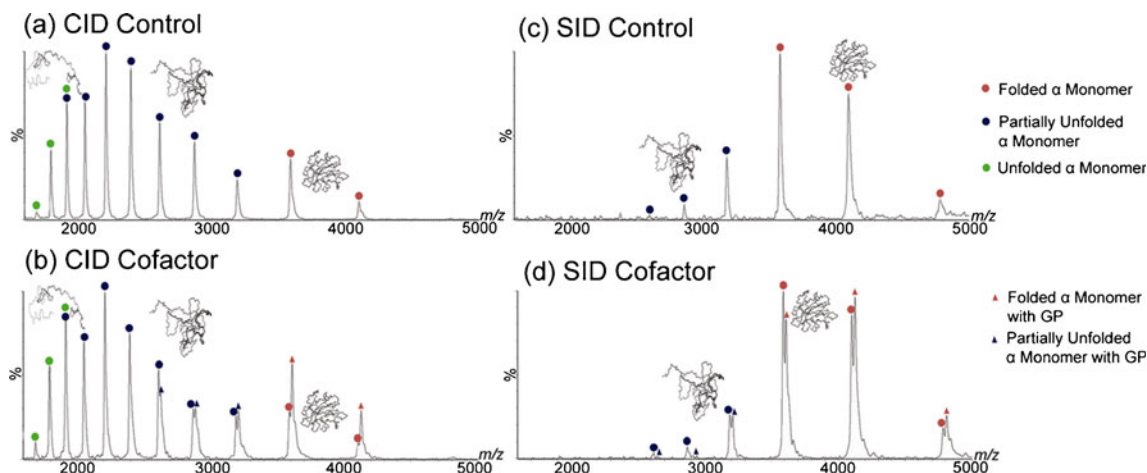


**Fig. 5** Monomer products of the +27 precursor of TS both with and without a ligand. Nano-ESI MS/MS control spectra in (a) and (c) were obtained by spraying 100  $\mu$ M TS and 20 mM L-Serine in 100 mM  $\text{NH}_4\text{OAc}$ ; while cofactor spectra (b) and (d) were obtained by spraying 100  $\mu$ M TS, in 100 mM  $\text{NH}_4\text{OAc}$  (which contained 20 mM L-Serine

and 40mM GP) at an acceleration voltage of 100 V in both CID and SID. In (b) and (d) peak doublets are indicative of two populations, one of which is ligand-containing. A comparison of spectra at various charge states shows that ligand is present only in folded and partially folded monomers

present, shows that in CID only some peaks exist as doublets, whereas in SID all  $\alpha$ -monomer peaks are present as doublets. These results further indicate that more SID product ions that are in their “native-like” states survived as manifested by the preservation of the ligand adducts, as compared to CID product-ions which exist predominantly in the unfolded state.

## Conclusions

The investigation of a hetero-tetrameric complex offers an opportunity to gain insight into the effects of structural features on the dissociation of complexes using different activation methods. The findings of such an investigation are summarized in Fig. 1, where it is evident that CID leads to significant unfolding of the monomer subunit and its separation from the remaining (n-1)mer. However, SID is a higher-energy, fast process that deposits more energy into the complex therefore resulting in more dissociation products than CID. In this present study, we also show that SID products are more “native-like”, i.e. have CCS consistent with crystal structure, than those obtained from CID and thus SID offers more topological information on the structure of protein complexes.

In this work, we measured the unfolding of undissociated precursor in CID along with ion mobility drift times, to investigate the unfolding of the Tryptophan Synthase complex. Here we show that the  $\alpha$ -monomer, when present on both the tetramer and trimer, behaves similarly to when it is present as a single entity, undergoing multistate unfolding.

The fact that in this experiment we were able to vary the acceleration voltage and hence the collision energy in CID, coupled with the ability of IM to separate product ions of similar  $m/z$  having different conformations allowed us to identify three stable intermediates and propose the steps of unfolding of the TS complex.

In the final part of this study, we were able to utilize the ability of IM to monitor conformational changes to investigate the effect of adding a ligand to a protein complex. Here, IM-MS fingerprint experiments revealed that upon addition of GP, not only is a conformational change observed, but also the “native-like” state of the tetrameric TS complex is more stable. Both CID and SID activation revealed that GP was buried within the  $\alpha$ -monomer, as it could only be found in either the folded or partially folded conformers of the  $\alpha$ -monomer.

**Acknowledgments** We are grateful for financial support from the National Science Foundation (NSF DBI 0923551 to VHW). We thank Sarah Fegan and Dr. Mark Thachuk (University of British Columbia, Canada) for helpful discussions and sharing of some preliminary simulation data of the TS tetramer unfolding. An allocation of computer time from the UA Research Computing High Performance Computing (HTC) and High Throughput Computing (HTC) at the University of Arizona is gratefully acknowledged.

## References

1. Ajay, Murcko MA (1995) Computational methods to predict binding free energy in ligand-receptor complexes. *J Med Chem* 38(26):4953–4967. doi:10.1021/jm00026a001
2. Bartholmes P, Teuscher B (1979) Cooperative binding of  $\alpha$  subunits to the Apo- $\beta$ 2 subunit of tryptophan synthase from

- Escherichia coli. *Eur J Biochem* 95(2):323–326. doi:10.1111/j.1432-1033.1979.tb12968.x
3. Beardsley RL, Jones CM, Galhena AS, Wysocki VH (2009) Noncovalent protein tetramers and pentamers with “n” charges yield monomers with n/4 and n/5 charges. *Anal Chem* 81(4):1347–1356. doi:10.1021/ac801883k
  4. Benesch JLP (2009) Collisional activation of protein complexes: picking up the pieces. *J Am Soc Mass Spectrom* 20(3):341–348. doi:10.1016/j.jasms.2008.11.014
  5. Benesch JLP, Sobott F, Robinson CV (2003) Thermal dissociation of multimeric protein complexes by using nano-electrospray mass spectrometry. *Anal Chem* 75(10):2208–2214. doi:10.1021/ac034132x
  6. Blackwell AE, Dodds ED, Bandarian V, Wysocki VH (2011) Revealing the quaternary structure of a heterogeneous noncovalent protein complex through surface-induced dissociation. *Anal Chem* 83(8):2862–2865. doi:10.1021/ac200452b
  7. Bornschein R, Hyung S-J, Ruotolo B (2011) Ion mobility-mass spectrometry reveals conformational changes in charge reduced multiprotein complexes. *J Am Soc Mass Spectrom* 22(10):1690–1698. doi:10.1007/s13361-011-0204-y
  8. Brändén C-I (1991) The TIM barrel—the most frequently occurring folding motif in proteins: Current Opinion in Structural Biology 1991, 1:978–983. *Curr Opin Struct Biol* 1(6):978–983. doi:10.1016/0959-440x(91)90094-a
  9. Brandts JF, Hu CQ, Lin LN, Mas MT (1989) A simple model for proteins with interacting domains. Applications to scanning calorimetry data. *Biochemistry* 28(21):8588–8596. doi:10.1021/bi00447a048
  10. Bush MF, Hall Z, Giles K, Hoyes J, Robinson CV, Ruotolo BT (2010) Collision cross sections of proteins and their complexes: a calibration framework and database for gas-phase structural biology. *Anal Chem* 82:9557–9565. doi:10.1021/ac1022953
  11. Christensen H, Pain RH (1991) Molten globule intermediates and protein folding. *Eur Biophys J* 19(5):221–229. doi:10.1007/bf00183530
  12. Creighton TE (1990) Protein folding. *Biochem J* 270(1):1–16
  13. Djavadi-Ohanian L, Friguet B, Goldberg ME (1986) Conformational effects of ligand binding on the beta.2 subunit of Escherichia coli tryptophan-synthase analyzed with monoclonal antibodies. *Biochemistry* 25(9):2502–2508. doi:10.1021/bi00357a033
  14. Dodds ED, Blackwell AE, Jones CM, Holso KL, O'Brien DJ, Cordes MHJ, Wysocki VH (2011) Determinants of gas-phase disassembly behavior in homodimeric protein complexes with related yet divergent structures. *Anal Chem* 83(10):3881–3889. doi:10.1021/ac2003906
  15. Dunn MF, Nix D, Ngo H, Barends TRM, Schlichting I (2008) Tryptophan synthase: the workings of a channeling nanomachine. *Trends Biochem Sci* 33(6):254–264. doi:10.1016/j.tibs.2008.04.008
  16. Erba EB, Ruotolo BT, Barsky D, Robinson CV (2010) Ion mobility-mass spectrometry reveals the influence of subunit packing and charge on the dissociation of multiprotein complexes. *Anal Chem* 82(23):9702–9710. doi:10.1021/ac101778e
  17. Farber GK (1993) An  $\alpha/\beta$ -barrel full of evolutionary trouble. *Curr Opin Struct Biol* 3(3):409–412. doi:10.1016/s0959-440x(05)80114-9
  18. Farber GK, Petsko GA (1990) The evolution of  $\alpha/\beta$  barrel enzymes. *Trends Biochem Sci* 15(6):228–234. doi:10.1016/0968-0004(90)90035-a
  19. Fenn J, Mann M, Meng C, Wong S, Whitehouse C (1989) Electrospray ionization for mass spectrometry of large biomolecules. *Science* 246(4926):64–71. doi:10.1126/science.2675315
  20. Finke JM, Onuchic JN (2005) Equilibrium and kinetic folding pathways of a TIM barrel with a funneled energy landscape. *Biophys J* 89(1):488–505. doi:10.1529/biophysj.105.059147
  21. Freeke J, Bush MF, Robinson CV, Ruotolo BT (2012) Gas-phase protein assemblies: unfolding landscapes and preserving native-like structures using noncovalent adducts. *Chem Phys Lett* 524:1–9. doi:10.1016/j.cplett.2011.11.014
  22. Freeke J, Robinson CV, Ruotolo BT (2010) Residual counter ions can stabilise a large protein complex in the gas phase. *Int J Mass Spectrom* 298(1–3):91–98. doi:10.1016/j.ijms.2009.08.001
  23. Galhena AS, Dagan S, Jones CM, Beardsley RL, Wysocki VH (2008) Surface-induced dissociation of peptides and protein complexes in a quadrupole/time-of-flight mass spectrometer. *Anal Chem* 80(5):1425–1436. doi:10.1021/ac701782q
  24. Gething M-J, Sambrook J (1992) Protein folding in the cell. *Nature* 355(6355):33–45
  25. Griko YV, Venyaminov SY, Privalov PL (1989) Heat and cold denaturation of phosphoglycerate kinase (interaction of domains). *FEBS Lett* 244(2):276–278. doi:10.1016/0014-5793(89)80544-7
  26. Hartl FU (1996) Molecular chaperones in cellular protein folding. *Nature* 381(6583):571–580
  27. Heck AJR (2008) Native mass spectrometry: a bridge between interactomics and structural biology. *Nat Meth* 5(11):927–933
  28. Hernandez H, Robinson CV (2007) Determining the stoichiometry and interactions of macromolecular assemblies from mass spectrometry. *Nat Protocols* 2(3):715–726
  29. Hilton GR, Benesch JLP (2012) Two decades of studying non-covalent biomolecular assemblies by means of electrospray ionization mass spectrometry. *J R Soc Interface* 9(70):801–816. doi:10.1098/rsif.2011.0823
  30. Hyde CC, Ahmed SA, Padlan EA, Miles EW, Davies DR (1988) Three-dimensional structure of the tryptophan synthase alpha 2 beta 2 multienzyme complex from Salmonella typhimurium. *J Biol Chem* 263(33):17857–17871
  31. Hyung S-J, Robinson CV, Ruotolo BT (2009) Gas-phase unfolding and disassembly reveals stability differences in ligand-bound multiprotein complexes. *Chem Biol* 16(4):382–390. doi:10.1016/j.chembiol.2009.02.008
  32. Jones CM, Beardsley RL, Galhena AS, Dagan S, Cheng G, Wysocki VH (2006) Symmetrical gas-phase dissociation of noncovalent protein complexes via surface collisions. *J Am Chem Soc* 128(47):15044–15045. doi:10.1021/ja064586m
  33. Jurneczko E, Barran PE (2011) How useful is ion mobility mass spectrometry for structural biology? The relationship between protein crystal structures and their collision cross sections in the gas phase. *Analyst* 136(1):20–28
  34. Kim PS, Baldwin RL (1982) Specific intermediates in the folding reactions of small proteins and the mechanism of protein folding. *Annu Rev Biochem* 51(1):459–489. doi:10.1146/annurev.bi.51.070182.002331
  35. Kirschner K, Wiskocil RL, Foehn M, Rezeau L (1975) The tryptophan synthase from Escherichia coli. *Eur J Biochem* 60(2):513–523. doi:10.1111/j.1432-1033.1975.tb21030.x
  36. Law R, Harper S, Speicher DW, Discher DE (2004) Influence of lateral association on forced unfolding of antiparallel spectrin heterodimers. *J Biol Chem* 279(16):16410–16416. doi:10.1074/jbc.M313107200
  37. Levinthal C (1968) Are there pathways for protein folding? *J Chim Phys* 65:44–45
  38. Levy ED, Erba EB, Robinson CV, Teichmann SA (2008) Assembly reflects evolution of protein complexes. *Nature* 453 (7199):1262–1265. [http://www.nature.com/nature/journal/v453/n7199/supinfo/nature06942\\_S1.html](http://www.nature.com/nature/journal/v453/n7199/supinfo/nature06942_S1.html)
  39. Loo JA, Berhane B, Kaddis CS, Wooding KM, Xie Y, Kaufman SL, Chernushevich IV (2005) Electrospray ionization mass spectrometry and ion mobility analysis of the 20S proteasome complex. *J Am Soc Mass Spectrom* 16(7):998–1008. doi:10.1016/j.jasms.2005.02.017

40. Matthews CR, Crisanti MM (1981) Urea-induced unfolding of the  $\alpha$ -subunit of tryptophan synthase: evidence for a multistate process. *Biochemistry* 20(4):784–792. doi:10.1021/bi00507a021
41. Mesleh MF, Hunter JM, Shvartsburg AA, Schatz GC, Jarrold MF (1996) Structural information from ion mobility measurements: effects of the long-range potential. *J Phys Chem* 100(40):16082–16086. doi:10.1021/jp961623v
42. Michael L (1976) A simplified representation of protein conformations for rapid simulation of protein folding
43. Miles EW, Rhee S, Davies DR (1999) The molecular basis of substrate channeling. *J Biol Chem* 274(18):12193–12196. doi:10.1074/jbc.274.18.12193
44. Ngo H, Harris R, Kimmich N, Casino P, Niks D, Blumenstein L, Barends TR, Kulik V, Weyand M, Schlichting I, Dunn MF (2007) Synthesis and characterization of allosteric probes of substrate channeling in the tryptophan synthase holoenzyme complex $\dagger, \ddagger$ . *Biochemistry* 46(26):7713–7727. doi:10.1021/bi700385f
45. Ngo H, Kimmich N, Harris R, Niks D, Blumenstein L, Kulik V, Barends TR, Schlichting I, Dunn MF (2007) Allosteric regulation of substrate channeling in tryptophan synthase: modulation of the l-Serine reaction in stage I of the  $\beta$ -reaction by  $\alpha$ -site ligands $\dagger, \ddagger$ . *Biochemistry* 46(26):7740–7753. doi:10.1021/bi7003872
46. Nicholls A, Sharp KA, Honig B (1991) Protein folding and association: insights from the interfacial and thermodynamic properties of hydrocarbons. *Proteins* 11(4):281–296. doi:10.1002/prot.340110407
47. Pagel K, Hyung S-J, Ruotolo BT, Robinson CV (2010) Alternate dissociation pathways identified in charge-reduced protein complex ions. *Anal Chem* 82(12):5363–5372. doi:10.1021/ac101121r
48. Peschke M, Verkerk UH, Kebarle P (2004) Features of the ESI mechanism that affect the observation of multiply charged noncovalent protein complexes and the determination of the association constant by the titration method. *J Am Soc Mass Spectrom* 15(10):1424–1434. doi:10.1016/j.jasms.2004.05.005
49. Politis A, Park AY, Hyung S-J, Barsky D, Ruotolo BT, Robinson CV (2010) Integrating ion mobility mass spectrometry with molecular modelling to determine the architecture of multiprotein complexes. *PLoS One* 5(8):e12080. doi:10.1371/journal.pone.0012080
50. Privalov PL (1982) Stability of proteins: proteins which do not present a single cooperative system. *Adv Protein Chem.* 35:1–104. doi:10.1016/S0065-3233(08)60468-4
51. Raboni S, Bettati S, Mozzarelli A (2009) Tryptophan synthase: a mine for enzymologists. *Cell Mol Life Sci* 66(14):2391–2403. doi:10.1007/s00018-009-0028-0
52. Remeta DP, Miles EW, Gisburg A (1995) Thermally induced unfolding of the tryptophan synthase  $\alpha 2\beta 2$  multienzyme complex from *Salmonella typhimurium*. *Pure Appl Chem* 67(11):1859–1866
53. Rhee S, Parris KD, Hyde CC, Ahmed SA, Miles EW, Davies DR (1997) Crystal structures of a mutant ( $\beta$ K87T) tryptophan synthase  $\alpha 2\beta 2$  complex with ligands bound to the active sites of the  $\alpha$ - and  $\beta$ -subunits reveal ligand-induced conformational changes $\ddagger$ . *Biochemistry* 36(25):7664–7680. doi:10.1021/bi9700429
54. Rojsajjakul T, Wintrode P, Vadrevu R, Robert Matthews C, Smith DL (2004) Multi-state unfolding of the  $\alpha$  subunit of tryptophan synthase, a TIM barrel protein: insights into the secondary structure of the stable equilibrium intermediates by hydrogen exchange mass spectrometry. *J Mol Biol* 341(1):241–253. doi:10.1016/j.jmb.2004.05.062
55. Ruotolo BT, Benesch JLP, Sandercock AM, Hyung S-J, Robinson CV (2008) Ion mobility-mass spectrometry analysis of large protein complexes. *Nat Protocols* 3(7):1139–1152
56. Ruotolo BT, Giles K, Campuzano I, Sandercock AM, Bateman RH, Robinson CV (2005) Evidence for macromolecular protein rings in the absence of bulk water. *Science* 310(5754):1658–1661. doi:10.1126/science.1120177
57. Ruotolo BT, Hyung S-J, Robinson PM, Giles K, Bateman RH, Robinson CV (2007) Ion mobility-mass spectrometry reveals long-lived, unfolded intermediates in the dissociation of protein complexes. *Angew Chem Int Ed* 46(42):8001–8004. doi:10.1002/anie.200702161
58. Ruotolo BT, Robinson CV (2006) Aspects of native proteins are retained in vacuum. *Curr Opin Chem Biol* 10(5):402–408. doi:10.1016/j.cbpa.2006.08.020
59. Ruvinov SB, Yang X-J, Parris KD, Banik U, Ahmed SA, Miles EW, Sackett DL (1995) Ligand-mediated changes in the tryptophan synthase indole tunnel probed by Nile red fluorescence with wild type, mutant, and chemically modified enzymes. *J Biol Chem* 270(11):6357–6369. doi:10.1074/jbc.270.11.6357
60. Salbo R, Bush MF, Naver H, Campuzano I, Robinson CV, Pettersson I, Jørgensen TJD, Haselmann KF (2012) Traveling-wave ion mobility mass spectrometry of protein complexes: accurate calibrated collision cross-sections of human insulin oligomers. *Rapid Commun Mass Spectrom* 26:1181–1193. doi:10.1002/rcm.6211
61. Sharon M (2010) How far can we go with structural mass spectrometry of protein complexes? *J Am Soc Mass Spectrom* 21(4):487–500. doi:10.1016/j.jasms.2009.12.017
62. Smith A (2003) Protein misfolding. *Nature* 426(6968):883–883
63. Stengel F, Baldwin Andrew J, Bush Matthew F, Hilton Gillian R, Lioe H, Basha E, Jaya N, Vierling E, Benesch Justin LP (2012) Dissecting heterogeneous molecular chaperone complexes using a mass spectrum deconvolution approach. *Chem Biol* 19(5):599–607
64. van den Heuvel RHH, van Duijn E, Mazon H, Synowsky SA, Lorenzen K, Versluis C, Brouns SJJ, Langridge D, van der Oost J, Hoyes J, Heck AJR (2006) Improving the performance of a quadrupole time-of-flight instrument for macromolecular mass spectrometry. *Anal Chem* 78(21):7473–7483. doi:10.1021/ac061039a
65. Wierenga RK (2001) The TIM-barrel fold: a versatile framework for efficient enzymes. *FEBS Lett* 492(3):193–198
66. Wilm M, Mann M (1996) Analytical properties of the nanoelectrospray ion source. *Anal Chem* 68(1):1–8. doi:10.1021/ac9509519
67. Wintrode PL, Rojsajjakul T, Vadrevu R, Matthews CR, Smith DL (2005) An obligatory intermediate controls the folding of the  $\alpha$ -subunit of tryptophan synthase, a TIM barrel protein. *J Mol Biol* 347(5):911–919. doi:10.1016/j.jmb.2005.01.064
68. Wysocki VH, Jones CM, Galhena AS, Blackwell AE (2008) Surface-induced dissociation shows potential to be more informative than collision-induced dissociation for structural studies of large systems. *J Am Soc Mass Spectrom* 19(7):903–913. doi:10.1016/j.jasms.2008.04.026
69. Zhou M, Dagan S, Wysocki VH (2012) Protein subunits released by surface collisions of noncovalent complexes: natively compact structures revealed by ion mobility mass spectrometry. *Angew Chem Int Ed* 51(18):4336–4339. doi:10.1002/anie.201108700